A Hybrid Algorithm Introducing Cross Mutation and Non-linear Learning Factor for Optimal Allocation of DGs and Minimizing Annual Network Loss in the Distribution Network

Gonggui Chen, *Member, IAENG*, Shitao Li, Hongyu Long*, Xianjun Zeng, Peng Kang,and Jinming Zhang

***Abstract*—Distributed generators (DGs) are recognized as an effective method for controlling the power loss, voltage stability, etc.. In this paper, a novel hybrid algorithm of beetle antennae search (BAS) and particle swarm optimization (PSO) is presented for optimal allocation of DGs in radial distribution network. The BAS describes the beetle's individual search by smell, PSO describes the group search of birds by location. The proposed algorithm combines their advantages, proceeds with individual optimization while conducting group optimization. Therefore, the proposed algorithm searches widely, and converges fast. In this paper, a series of improvement measures are proposed to deal with the shortcoming of PSO-BAS which is easy to fall into local optimum. These methods include equal interval initialization, cross mutation, and non-linear learning factor. This paper will show the comparison results of PSO-BAS and IPSO-BAS in the six confessed test functions to prove the necessity of the improved methods. Simultaneously, in order to verify the feasibility and effectiveness of this proposed algorithm in terms of practical application, it is tested on the standard IEEE 33-bus, IEEE 69-bus and IEEE 119-bus systems. The results of active power loss and voltage stability show that proposed algorithm is more effective and more suitable for the power distribution system than other algorithms. At the same time, this article also explores the impact of new energy sources on the annual network loss. Besides, a method for optimizing the annual network loss is proposed. Here, the IPSO-BAS algorithm is used to adjust the size of multiple biomass energy sources within 24 hours to optimize the network loss, and a comparison plan is designed to verify the feasibility of the proposed method. According to the final result, this proposed method can greatly reduce the annual network loss.**

***Index Terms*—distributed generators (DGs), improvement measures, hybrid algorithm, new energy, annual network loss.**

Manuscript received December 15, 2020; revised May 18, 2021. This work was supported by the National Natural Science Foundation of China under Grant 51207064.

Gonggui Chen is a professor of Key Laboratory of Industrial Internet of Things and Networked Control, Ministry of Education, Chongqing University of Posts and Telecommunications, Chongqing 400065, China; Chongqing Key Laboratory of Complex Systems and Bionic Control, Chongqing University of Posts and Telecommunications, Chongqing 400065, China (e-mail: chenggpower@ 126.com).

Shitao Li is a master degree candidate of Chongqing Key Laboratory of Complex Systems and Bionic Control, Chongqing University of Posts and Telecommunications, Chongqing 400065, China (e-mail: lstcqupt@163.com).

Hongyu Long is a senior engineer of Chongqing Key Laboratory of Complex Systems and Bionic Control, Chongqing University of Posts and Telecommunications, Chongqing 400065, China (corresponding author to provide phone: +8613996108500; e-mail: longhongyu20@163.com).

Xianjun Zeng is a senior engineer of State Grid Chongqing Electric Power Company, Chongqing 400015, China (e-mail: 13594255525@139.com).

Peng Kang is a senior engineer of Economic and Technology Research Institute, State Grid Chongqing Electric Power Company, Chongqing 401120, China (e-mail: 1060846892@qq.com).

Jinming Zhang is a senior engineer of State Grid Chongqing Electric Power Company, Chongqing 400015, China (e-mail: zjm213@163.com).

I. Introduction

MODERN large-scale power distribution network is constantly facing an ever-growing load demand. Therefore, the distribution network gradually becomes more complex than before. At the same time, there are also plenty of problems such as the power loss, voltage stability, etc.. In order to solve these problems, distributed generators (DGs) [1] were proposed, DGs have qualitatively improved this problem. Usually, the distributed generators are installed in a radial distribution network [2, 3]. Among many feasible devices, because DGs can provide both active and reactive power, they have many applications in the distribution system. Besides, people began to vigorously promote renewable energy as a distributed power source in modern times. This article explores that the optimal network loss is caused by renewable energies under the 24-hour daily load curve. For renewable energy, this article proposes three types, called wind energy, solar energy and biomass energy. Among them, biomass energy is the most flexible, and the other two energy sources are restricted by natural factors.

Consequently, the ODGA (Optimal DG Allocation) is critical. Here is a method to reduce the power loss, enhance voltage stability by adjusting the location and size of DGs. Hence, the optimal location and size of DGs are necessary tasks for this paper.

In order to achieve the optimal allocation of DGs in a radial distribution network, there is a large amount of literature that has conducted in-depth research on this optimization problem. In literature [4], particle swarm optimization (PSO) decides the optimal allocation and penetration of wind DGs in the distribution network in order to minimize the Average Multi-Objective Index (AIMO), here is a kind of renewable energy (wind DGs) and a new evaluation index, which put forward a new direction for the sustainable development and stability evaluation of the power system. In literature [5], the PGSA has been modified and simulations have been carried out to prove the advantages of the proposed algorithm (MPGSA) of faster convergence. PGSA is based on the plant growth process, and the root is the initial point of growth. Similar to initialization, the main stem and branches grow. Starting from the node is like searching for the best value, this article puts forward a new point of view, which roughly converts static power into dynamic power. Moradi and Abedini proposed the GA/PSO algorithm, which is a fusion of GA and PSO, and the algorithm can significantly reduce the network loss and improve the voltage stability by adjusting the position and size of DGs on the IEEE 33-bus and IEEE 69-bus systems. Because the two algorithms have their own characteristics, it is a reasonable method to combine them. Compared with PSO and GA, its performance is significantly improved, but it still cannot get an excellent result [6]. Kumar and Kumar proposed loss sensitivity factor simulated annealing (LSFSA) in order to explore the potential for the optimal size and location of the DGs. LSFSA has extremely high performance on low-dimensional problem, but the complexity of the problem increases, the performance of LSFSA gradually deteriorates [7]. Aiming at the joint execution of the Grasshopper Optimization Algorithm (GOA) and Cuckoo Search (CS), a hybrid technique is proposed, which determines the ideal position of the DG unit in terms of power loss, line flow, and voltage, this technique perfectly combines the two bionic algorithms by their biological characteristics, and the performance has been greatly improved, this technique provides a new idea for the fusion of algorithms [8]. Hybrid algorithm (DE-PS) is used as a meta-heuristic optimization tool to solve the best capacitor location problem and to estimate the optimal parallel capacitor compensation level/size required to reduce line power loss within voltage constraints, this hybrid algorithm provides more ideas for algorithm fusion thinking by fusing two mathematical thinking algorithms [9]. In literature [10], the basic shortcoming of the original teaching-learning-based optimization algorithm (TLBO) is that it provides a near-optimal solution within a limited iteration period, rather than an optimal solution. Distributed generators have an overall positive impact on distribution system, although this algorithm only provides a fast iterative idea, its core essence can be integrated into other algorithms and improve its performance. In literature [11], a novel method about the combination of the Genetic Algorithm (GA) and Intelligent Water Drops (IWD) is proposed to find the suitable location and size of DGs to minimize the system power loss, improve the voltage regulation and voltage stability within constraints of the distribution system. This algorithm combines biological genetic characteristics and natural characteristics. It has better performance than GA/PSO, but it cannot also get excellent results. In literature [12], three kinds of renewable energy (biomass, wind and photovoltaic) are applied to the distribution network, and a method is proposed to adjust the energy size to obtain the minimum energy loss for every year, and this article provides more methods for the sustainable development of distribution power generation and initially transforms the static system loss to the dynamic system loss.

In this article, a hybrid algorithm (PSO-BAS) is proposed here. The main reason for choosing the two algorithms is that the two algorithms are the group search and individual search. PSO-BAS perfectly combines these two algorithms biological characteristics and core ideas. Compared with PSO, PSO-BAS's performance has been greatly improved, and it has better performance on high-dimensional issues. In the second section of this article, here is a list of constraint formulas for each indicator of the power system, and the algorithm is strictly designed by these constraints. In the third section, here is a brief introduction to the PSO and BAS algorithms, and this section focuses on the PSO-BAS algorithm flow and its pseudo-code. Since the algorithm may fall into a local optimum, here is a detailed explanation of the improvement method of the algorithm to obtain the IPSO-BAS, parameter optimization, crossover mutation, equal interval initialization, and nonlinear learning factor. In the fourth section of this article, IPSO-BAS is introduced into the IEEE 33-bus, IEEE 69-bus and IEEE 119-bus systems to obtain the optimal network active power loss, and it is found that IPSO-BAS will obtain faster convergence and broader search space over PSO-BAS, GA, PSO, GA/PSO, TLBO, GA-IWD, and LSFSA on high-dimensional system. In addition, this section also explores the insertion of renewable energy on the IEEE 69-bus system, and counts the active network loss for each hour. Here, a new method is proposed to minimize the annual network loss and initially convert the static network loss into a dynamic network loss. The last two sections of this article analyze and summarize the previous data, and show the IPSO-BAS is effective for obtaining the optimal network loss and the annual optimal network loss of the power system.

II. FORMULATION

The optimal locations and sizes of DG units are critical to reduce active power loss while satisfying all constrains of the distribution system [13-16].

A. Active power loss(P_L)

The active power loss is calculated as follows:

$$P_L = \sum_{k=1}^{N_L} R_k I_k^2 \tag{1}$$

where, R_k is the resistance of the *kth* branch, I_k is the current passing through the *kth* branch.

B. Minimize annual network loss

In this paper, it will also introduce new energy sources as distributed power sources, and discuss the practicability of new energy sources, and the corresponding formula for minimizing network loss each year is as follows:

$$MinE_{\mathrm{Loss}} = 365 * Min\sum_{i=1}^{24} P_{Loss}\left(i\right) * \Delta t \tag{2}$$

where, $P_{loss}(i)$ is the active power loss in the *ith* time interval, Δt is an hour.

C. Objective function

In order to prove whether the proposed algorithm is effective and suitable, this paper will analyze the results of the objective function, active power loss.

$$F = Min\left(P_L\right) \tag{3}$$

About the above objective function, this paper will proceed analysis and comparison of the calculation results between the improved algorithm and other algorithms under the same conditions of the power model.

D. System constrains

If the stable system can maintain running normally, it will be limited by various indicators. In this paper, the distribution network is subject to certain aspects, they are described by the following equalities and inequalities [17].

i. Load balance constraint

In this distribution network, each bus must be satisfied the constraints of power flow calculation as follows [18]:

$$P_{is} - e_i \sum_{j=1}^{n} \left(G_{ij} e_j - B_{ij} f_j \right) - f_i \sum_{j=1}^{n} \left(G_{ij} f_j + B_{ij} e_j \right) = 0 \quad (4)$$

$$Q_{is} - f_i \sum_{j=1}^{n} \left(G_{ij} e_j - B_{ij} f_j \right) + e_i \sum_{j=1}^{n} \left(G_{ij} f_j + B_{ij} e_j \right) = 0 \quad (5)$$

where, P_{is} and Q_{is} are the given active power and reactive power in the *ith* branch, e_i is the real part of the *ith* node voltage, f_i is the imaginary part of the *ith* node voltage, G_{ij} is the real part of the admittance between the *ith* and the *jth* branch, B_{ij} is the imaginary part of the admittance between the *ith* and the *jth* branch.

ii. Voltage limits

Each node voltage amplitude should be limited within the lower and upper bounds as follows:

$$V_{Min,i} \le V_i \le V_{Max,i} \quad (6)$$

where, $i=1,2,3 \ldots N_B$, $V_{Min,i}$ is the lowest voltage amplitude in the *ith* bus, $V_{Max,i}$ is the highest voltage amplitude in the *ith* bus.

iii. Current limits

Each branch current should not exceed the maximum limit as follows:

$$\left| I_k \right| \le \left| I_{Max,k} \right| \quad (7)$$

where, $k=1,2,3 \ldots N_L$, $I_{Max,k}$ is the maximun of the current in the *kth* branch.

iv. DG unit technical contraints

Here are some uniform limits about single DG in any given location, in order to make sure the DG working normally, any limit for DG should be maintain within the lower and upper bounds , DG capacity limit is as follows [19, 20]:

$$P_{Min,i}^{DG} \le P_i^{DG} \le P_{Max,i}^{DG} \quad (8)$$

$$Q_{Min,i}^{DG} \le Q_i^{DG} \le Q_{Max,i}^{DG} \quad (9)$$

where, $i=1,2,3 \ldots N_{DG}$, $P_{Min,i}^{DG}$ is the lowest active power limit of *ith* DG, $P_{Max,i}^{DG}$ is the highest active power limit of *ith* DG, $Q_{Min,i}^{DG}$ is the lowest reactive power limit of *ith* DG, $Q_{Max,i}^{DG}$ is the highest reactive power limit of *ith* DG.

DG power factor limit is as follows [21]:

$$pf_{Min,m}^{DG} \le pf_m^{DG} \le pf_{Max,m}^{DG} \quad (10)$$

where

$$pf_m^{DG} = \frac{P_m^{DG}}{\sqrt{\left(P_m^{DG}\right)^2 + \left(Q_m^{DG}\right)^2}} \quad (11)$$

$m=1,2,3 \ldots N_{DG}$, $pf_{Min,m}^{DG}$ is the lowest power factor of the *mth* DG, $pf_{Max,m}^{DG}$ is the highest power factor of the *mth* DG.

III. METHODOLOGY

A. Particle swarm optimization(PSO)

Particle Swarm Optimization (PSO) [22-27] was first proposed by Eberhart and Kennedy in 1995, and its basic concept stems from the research on the foraging behavior of birds.

A kind of particle is used to simulate the above bird individual. Each particle can be regarded as a search individual in the *N*-dimensional search space. The current position of the particle is a candidate solution for the corresponding optimization problem, and the flight process of the particle is the individual search process.

B. Beetle antennae search

Beetle Antennae Search (BAS) [28, 29], also called Beetle Antennae Search-BAS, is an efficient intelligent optimization algorithm proposed in 2017. Similar to other intelligent optimization algorithms such as genetic algorithm, particle swarm optimization, simulated annealing, etc., beetle search does not need to know the specific form of the function, and does not need gradient information to achieve efficient optimization.

Compared with particle swarm optimization, the beetle search requires only one individual, that is, one beetle, which greatly reduces the amount of calculation.

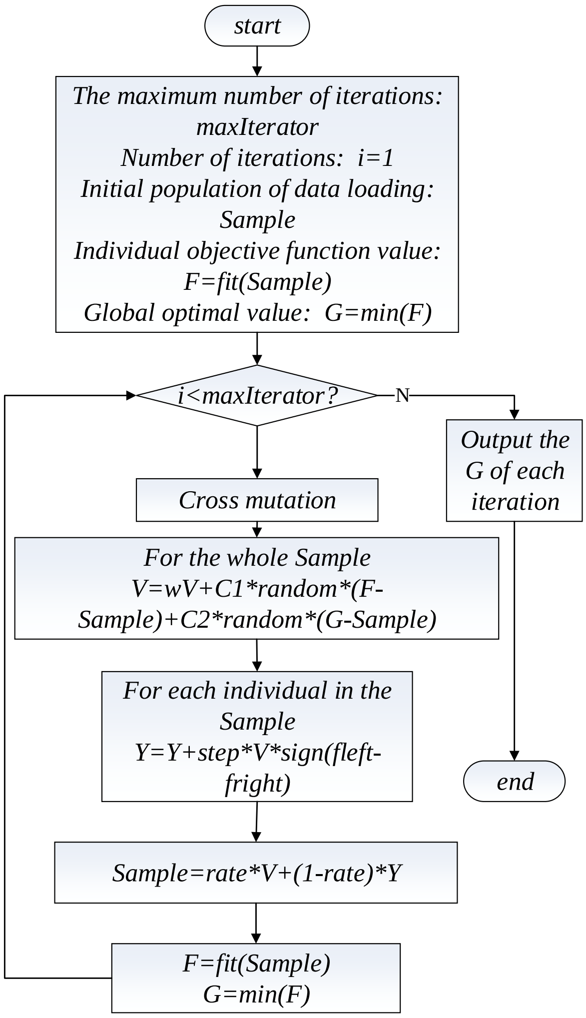

Fig.1 The flow chart of the IPSO-BAS

C. The hybrid algorithm of particle swarm optimization and beetle antennae search

The hybrid algorithm of particle swarm optimization and beetle antennae search (PSO-BAS) combines the advantages of both. PSO is a group optimization algorithm and BAS is an individual optimization algorithm. Whether it is from the perspective of mathematics or bionics, both are very suitable algorithms for combining the process of group optimization and individual optimization.

Step 1: Initialization

This method of initialization sets the number of initial population to 30 and limits the value range of each individual to the DG unit controllable range, then the maximum number of iterations is 100.

Step 2: Target value calculation

This step brings the initial value of the population into the fitness function *(fit)*, then it can get a series of the target values of the active power loss *(f_{loss})*, and take the smallest of all the calculated f_{loss} as the global optimal value *(g_{loss})*

$$f_{loss} = fit\left(value_{initial}\right) \tag{12}$$

$$g_{loss} = Min\left(f_{loss}\right) \tag{13}$$

Step 3: Group search

According to the PSO's group optimization rules, the next speed is obtained by the current speed and position, the local optimal position and the global optimal position.

$$V = wV + C1*r*(F - Sample) + C2*r*(G - Sample) \tag{14}$$

where, r is a random number from 0 to 1, F and G are the local optimal position and the global optimal position, The C_1 and C_2 are learning factors, *Sample* is the current position.

Step 4: Individual search

Through the individual optimization rules of the BAS, the individual searches the left and right optimal values one by one and uses the calculated speed to speed up the optimization when the position is updated.

$$Y = Y + step*V*sign(fit(left) - fit(right)) \tag{15}$$

where, *left* and *right* are the variables on the left and right.

Step 5: Location update

The individual search value and group search value above are added together in a certain proportion to obtain the final contemporary location value.Then, the current position value is brought into *fit* to get the f_{loss} and the minimum value g_{loss} for the next iteration is obtained by sorting from f_{loss}.

$$Sample = rate*V + (1 - rate)*Y \tag{16}$$

where, *rate* is a number from 0 to 1.

Step 6: Circular judgment

This step determines whether the current number of iterations reaches the maximum number of iterations, if not, jumps to *step 3*. Otherwise it outputs the global optimal value of each generation.

$$\begin{cases} iterations <= Max_{iterations} & step3 \\ iterations > Max_{iterations} & end \end{cases} \tag{17}$$

The flow chart of the PSO-BAS is shown in the Fig.1

D. Improved measure

i. Parameter optimization

The original PSO-BAS has achieved good results in terms of optimal allocation of DGs on the radial network. However, an improvement point will be introduced in order to make PSO-BAS to obtain faster convergence speed, broader search range, and does not fall into local optimum.

From pseudo code of the BAS, we can know the *eta* is a constant and it is set to 0.95 normally. If *eta* becomes a variable which is correlated with the number of iterations, this algorithm will get better performance as the increment for number of iterations in small-scale optimization. In the paper, *eta* is modified to a variable calculated by following formula (18):

$$eta = step_1 * \left(step_0 / step_1\right)^{\frac{maxIterator}{10*k+maxIterator}} \tag{18}$$

where, the *maxIterator* is the maximum number of iterations, k is the current iterations, $step_1$ and $step_0$ are the two constant values and they can quickly adjust the rate of change of *eta* through them.

ii. Cross mutation

Thoughts based on GA algorithm, an idea of cross mutation is introduced here.

Cross: when the current random probability is greater than the crossover probability, this method randomly takes two individuals to exchange partial value. (The preset cross probability value is generally 0.5~0.8)

$$P_i\left(1: pos\right) = P_j\left(1: pos\right) \tag{19}$$

$$P_j\left(pos+1: end\right) = P_i\left(pos+1: end\right) \tag{20}$$

where, $i \neq j$, but $i,j=1,2,3,4\ldots nSample$, *pos* is a random position between *1* and $MaxNumber_{DG}$ *(3 or 6)*, P_i is the *ith* individual in the population.

Mutation: before the mutation operation, a concentration calculation is introduced here to judge whether the particles are too concentrated in a certain range and may fall into the local optimum by the similarity between each individual.

Regarding the calculation of similarity, it is judged here how many identical variable values exist between each individual and other individuals. If the ratio of the same number reaches 0.7 or more, then the current individual similar concentration is added by 1, and finally the similar concentration coefficient formula is by following formula (21):

$$coe_{similar} = count_{similar} / \left(Sample - 1\right)^2 \tag{21}$$

where, $coe_{similar}$ is similar concentration coefficient, *Sample* is the number of population, $count_{similar}$ is individual similar concentration.

The mutation probability is proportional to $coe_{similar}$, and the formula is by following formula (22):

$$mu_P = mu_{Min} + (mu_{Max} - mu_{Min})*coe_{similar} \tag{22}$$

where, mu_p is the mutation probability, mu_{Min} is minimum value of the mutation probability, mu_{Max} is maximum value of the mutation probability. Here, the fitness is sorted into the last 10 populations, and the mutation operation is performed. The specific process is to randomly generate a variable from 0 to 1. If the current variable is less than the mutation probability (The preset mutation probability value is generally 0.1~0.4), then each selected individual will perform the following formula (23):

$$P_i\left(pos\right) = (max - min)*rand + min \tag{23}$$

where, *max* and *min* are the upper and lower limits of the value range, *rand* is a random number in the range 0~1.

Cross mutation is performed on the initial value of each iteration to expand its search range, avoid falling into local optimization, and improve the performance of PSO-BAS algorithm.

iii. Initialize the population at equal intervals

The intelligent optimization algorithm is very sensitive to the selection of the initial value, especially in a complex model, this phenomenon is more obvious, so an initial value selection method is proposed here to improve the search range and convergence speed of the algorithm. This method is called the equidistant method. As the name implies, when the population is initialized, each value of each population is evenly distributed within the whole ranges, so that the values of various sizes can be obtained as much as possible in the first value process. Besides, this method will prevent the algorithm from falling into a local optimum.

TABLE I SIX CONFESSED TEST FUNCTIONS

Test function	Ranges
$f_1(x)=\sum_{i=2}^{D}\left[100*\left(x_i-x_{i-1}^2\right)^2+\left(x_{i-1}-1\right)^2\right]$	$[-30,30]^D$
$f_2(x)=\sum_{i=1}^{D}\left(\lvert x_i+0.5\rvert^2\right)$	$[-100,100]^D$
$f_3(x)=\sum_{i=1}^{D}\left(i*x_i^4+rand\right)$	$[-1.28,1.28]^D$
$f_4(x)=\sum_{i=1}^{D}\left[-x_i*\sin\left(\sqrt{\lvert x_i\rvert}\right)\right]$	$[-500,500]^D$
$f_5(x)=-20*e^{-0.2*\sqrt{\left(\sum_{i=1}^{D}x_i^2\right)/D}}-e^{\left[\sum_{i=1}^{D}\cos(2*\pi*x_i)\right]/D}+20+e$	$[-32,32]^D$
$f_6(x)=\sum_{i=1}^{D}\lvert x_i\rvert+\prod_{1}^{D}\lvert x_i\rvert$	$[-50,50]^D$

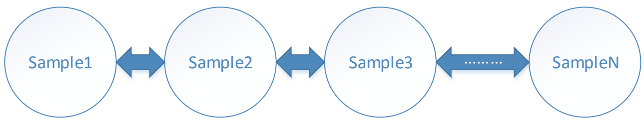

Fig.2 Initialize the population at equal intervals

In Fig.2, each circle represents a population, and it can be clearly observed that the distance between each circle is equal. The value of each population is by following formula (24):

$$Sample_i=\left[\cdots \quad x_{Min}+\left(x_{Max}-x_{Min}\right)*i/N\right] \tag{24}$$

where, *Sample* is the *ith* value of population, x_{Max} and x_{Min} are the maximum and minimum values of each dimension, N is the number of population.

iv. Non-linear learning factor

PSO-BAS has a fast convergence rate, this character will inevitably lead to a drawback, which is to fall into the local optimum. To further improve the algorithm, this article will introduce a non-linear learning factor.

In Fig.3, it shows the changing trend of C_1 and C_2.

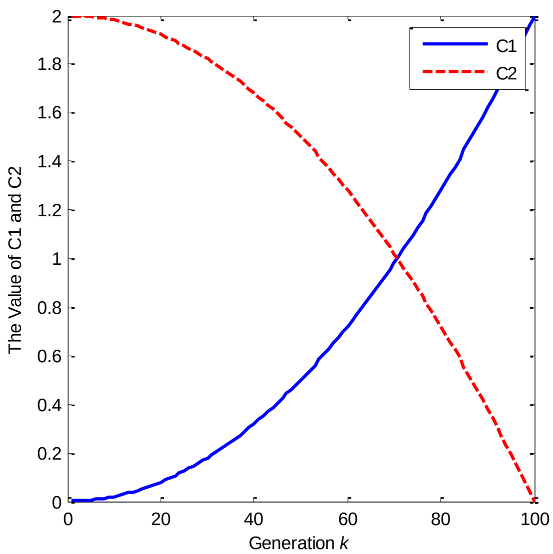

Fig.3 The changing trend of C_1 and C_2

About the non-linear learning factor, they will satisfy the following formula (25)-(26):

$$C_1=C\left(k^2/maxiterator^2\right) \tag{25}$$

$$C_2=C\left(1-k^2/maxiterator^2\right) \tag{26}$$

where, C is set to 2, *maxiterator* is the maximum number of iterations, k is the *kth* iteration. This method makes PSO-BAS bias towards global optimization in the early stage and partial optimization in the later stage.

Through these improvement measures, the search scheme of PSO-BAS has changed from a fixed step size to a progressive search in order to verify whether these measures achieve the effect of improvement. This paper will compare the results of PSO-BAS and improved algorithm (IPSO-BAS) on the IEEE 33-bus, IEEE 69-bus, IEEE 119-bus systems.

IV. Simulation and Analysis

First of all, we need to know whether the performance of the proposed hybrid algorithm has been improved by comparing its result with the consequence of original algorithm and whether the improved methods in this article are effective. Here, the PSO, PSO-BAS, and IPSO-BAS algorithms are simultaneously introduced into the six confessed test functions. About these test functions, here are a number of same conditions that need to be set, for example, the maximum number of iterations is set to 500, the dimension of initial population (D) is 30, the initial population is set to the same random population for PSO, PSO-BAS, IPSO-BAS.

The six confessed test functions will be shown in TABLE I.

The fitness value of the three algorithms in six confessed test functions can be observed in TABLE II, IPSO-BAS will chalk up the best results over PSO-BAS and PSO in all test functions, the proposed improvement methods are capable of making PSO-BAS get better performance by observing Fig.6-Fig.11. Except the value of $f_1(x)$, the results of PSO-BAS will be better than PSO. A conclusion that algorithm fusion and a series of necessary improvement methods will be obtained. This conclusion is not comprehensive, because the six test functions only exist on a theoretical level and do not consider the constraints of real physical conditions.

Therefore, in order to verify the superiority of the proposed improved algorithm in terms of practical application, it will be tested on the IEEE 33-bus, IEEE 69-bus, IEEE 119-bus systems and its results will be compared with other algorithms. In this paper, the IPSO-BAS algorithm based on the optimal DGs allocation of MATLAB codes is developed, and it is integrated together for simulation. At last, result data is obtained on the three models to verify the performance of IPSO-BAS. In this paper, two cases are proposed. About the case 1, the power factor is operated as unity (only supply active power for each generation). As for case 2, it is operated as 0.866 leading (supply active power and reactive power at the same time for each generation).

The simulation results are all based on MATLAB code to achieve. In all test models, the population of proposed IPSO-BAS is set to 30.

About IPSO-BAS, the initial value of each variable is as follows, the moving step (*step*) is equal to 500, constant for controlling step size (*c*) is equal to 2, the minimum initial step *($step_1$)* is equal to 0.4 and the maximum initial step *($step_0$)* is equal to 1.5.

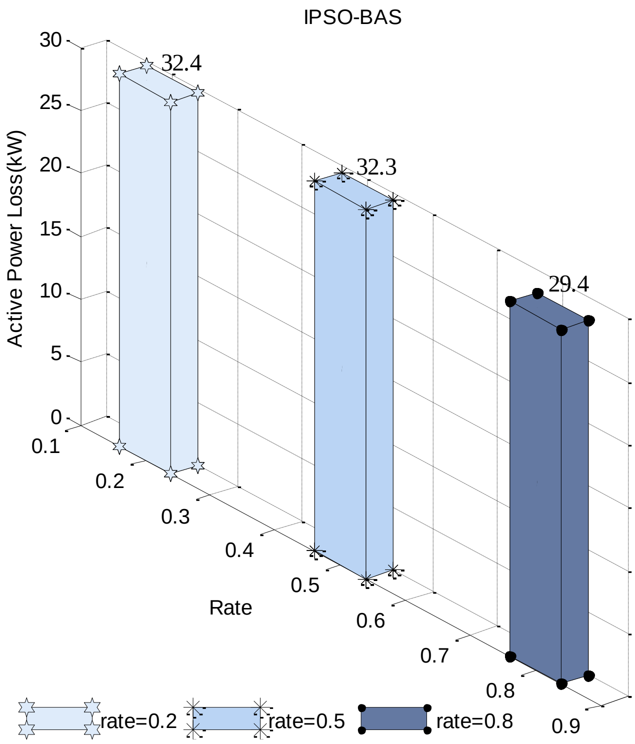

Fig.4 Active power loss using different rate for IPSO-BAS on the IEEE 33-bus system

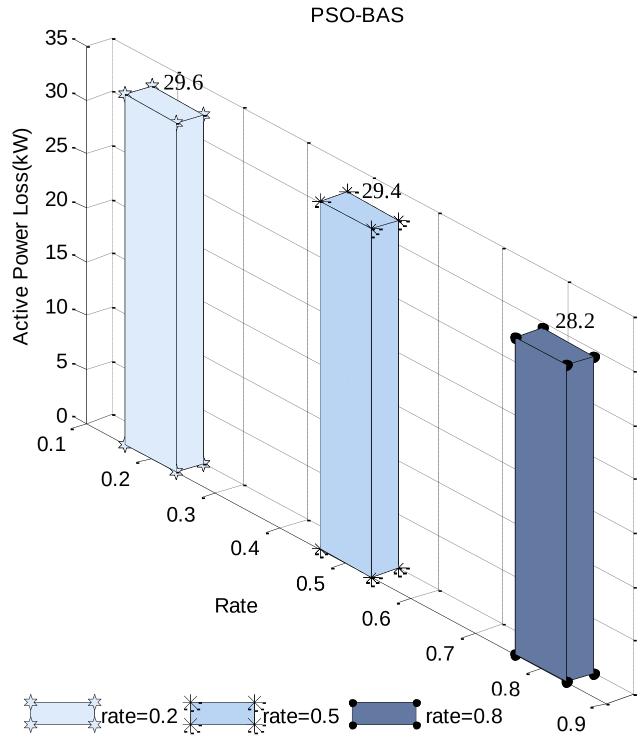

Fig.5 Active power loss using different rate for PSO-BAS on the IEEE 33-bus system

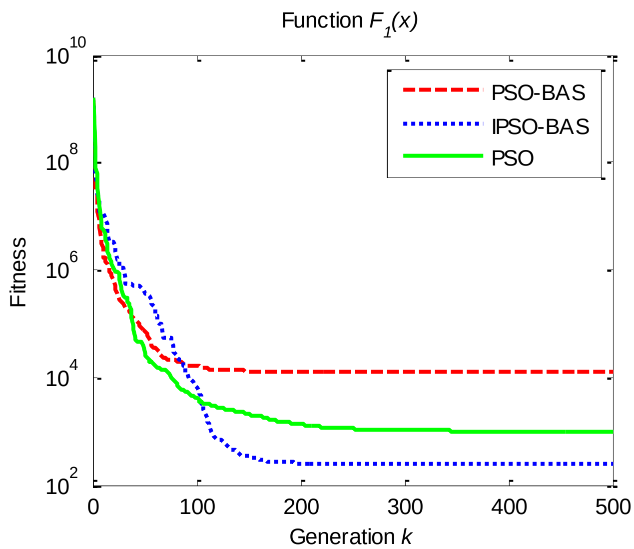

Fig.6 The iteration graph of $f_1(x)$

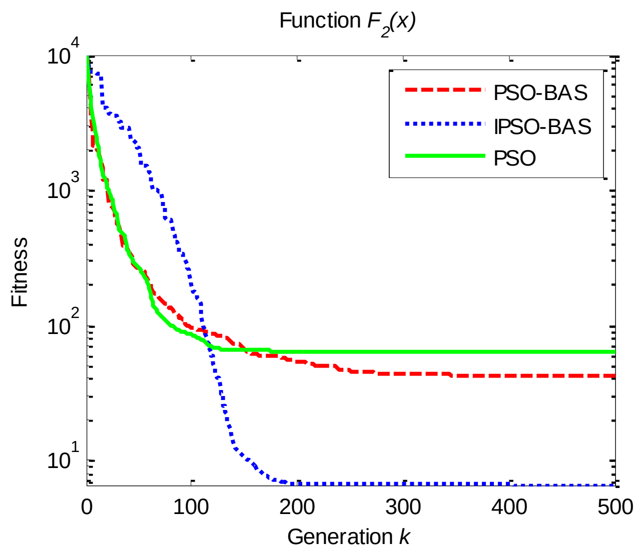

Fig.7 The iteration graph of $f_2(x)$

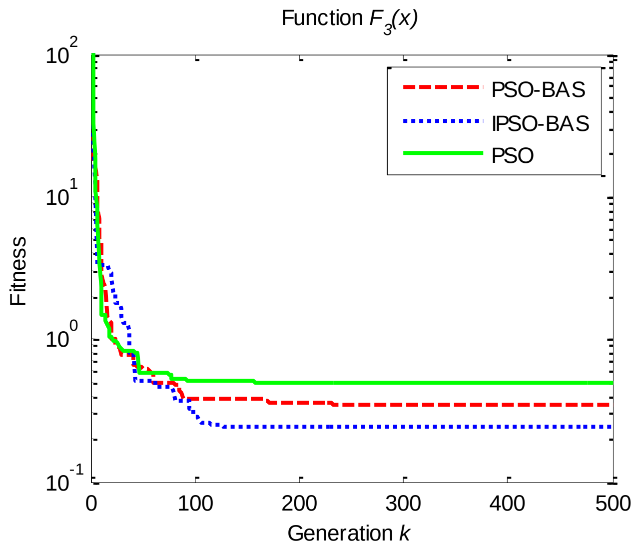

Fig.8 The iteration graph of $f_3(x)$

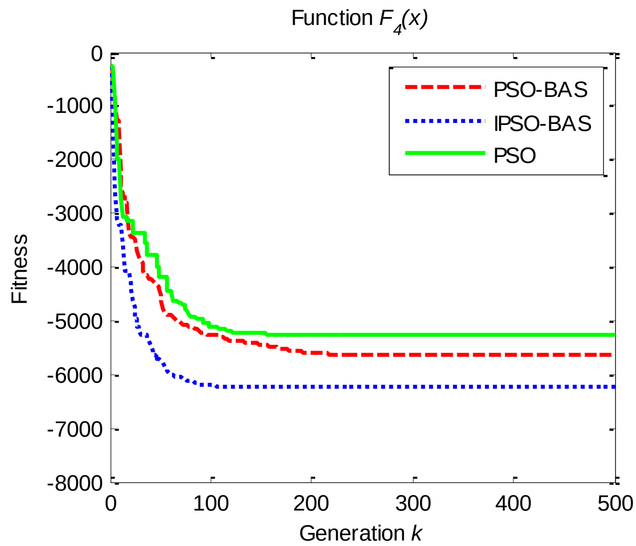

Fig.9 The iteration graph of $f_4(x)$

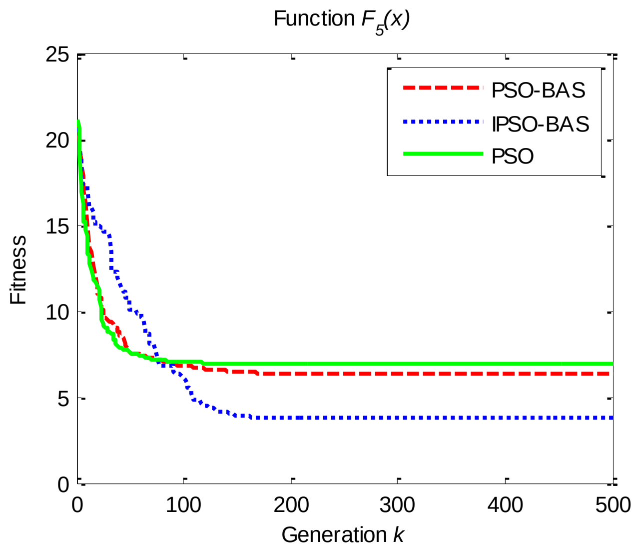

Fig.10The iteration graph of $f_5(x)$

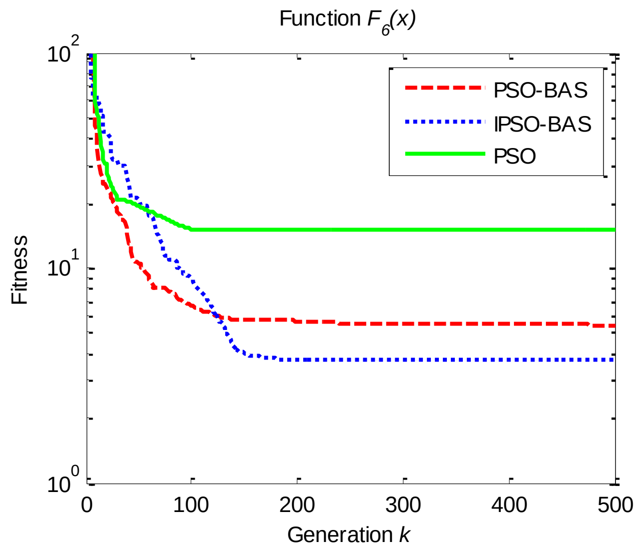

Fig.11The iteration graph of $f_6(x)$

TABLE II THE FITNESS VALUE OF THE THREE ALGORITHMS IN THE SIX CONFESSED TEST FUNCTIONS

Test function	IPSO-BAS	PSO-BAS	PSO
$f_1(x)$	251.01	12429	974.52
$f_2(x)$	6.56	41.87	63.04
$f_3(x)$	0.23	0.35	0.51
$f_4(x)$	-6360.53	-5440.75	-5276.38
$f_5(x)$	4.27	6.28	6.93
$f_6(x)$	3.88	5.75	12.12

A. IEEE 33-bus radial distribution system

In order to explore the performance of the algorithm on different models, here, the algorithm is first applied to the simpler IEEE 33-bus model for testing to verify how effective the algorithm is on low-dimensional data.

The maximum iteration of IPSO-BAS is set to 100 for case 1 and case 2. The line data and load data are given in [30]. The most important, when the power factor is 0.866 leading, it can be seen from Fig.4 that the proportion of fusion of two algorithms (*rate*=0.8) for IPSO-BAS gives the active power loss, 28.21kW. And in Fig.5, the same *rate* for PSO-BAS gives the active power loss, 29.42kW.

The distribution system has 33 nodes, and its nominal voltage is 12.66kV. The basic power value of the distribution system is 10MVA. The singline map about the distribution system is shown in Fig.24. The total load active power and reactive power of the distribution network are 3.715MW and 2.3MVar. The upper and lower voltage magnitude limits at all buses are 1.05 p.u. and 0.95 p.u., respectively. In order to ensure the fairness of the each algorithm, 3 DGs with the same parameter are uniformly accessed whether the power factor is unity or 0.866 leading [31-33].

The active power loss and reactive power loss of these radial distribution system are 210.998 kW and 143kVar without the installation of DGs. In order to prove the performance of these algorithms, DGs will be inserted into this distribution network to minimize active power loss. The ratings of DGs are set to the range of 0.5 p.u. to 1.2 p.u.. For each DG, their power factor will be set to unity and 0.866 leading.

The detailed results about the placement and the capacity of DGs, active power loss, critical bus number (CBN) and critical bus voltage (CBV) for two different cases (0.866 leading and unity) by different optimization algorithms are shown in TABLE III and TABLE IV.

Using the optimization performance of the algorithm, various algorithms can be found here to adjust the size of DGs to obtain the minimum system active power loss.

While the power factor is set to unity, various algorithms will get different results about active power loss in TABLE III. As the most classic optimization algorithm, the PSO has a strong convergence speed, which reduces the active power loss from 210.998kW to 105.35 kW [6], the 106.30 kW is obtained by GA [6], the active power loss of PSO/GA is 103.40 kW [6], the 82.03 kW is obtained by LSFSA [7], the 110.51 kW is obtained by the GA-IWD [11]. The TLBO obtains a smaller active power loss, 75.540 kW [10]. However, the PSO-BAS and IPSO-BAS can not obtain the best active power loss on the IEEE 33-bus radial distribution system, 90.21 kW and 89.40 kW. They are inferior to TLBO [10] and LSFSA [7]. On the other hand, when the power factor is set to 0.866 leading, 26.720 kW is obtained by the LSFSA [7], 29.42 kW is obtained by the PSO-BAS, 28.21 kW is obtained by IPSO-BAS.

It can be seen from the above data analysis that the same algorithm and different power factors have a huge gap in results, which also shows that DGs introduce reactive power, it will reduce the active power loss of the system to a greater extent. So for each DG, introduces active power and reactive power into power system at the same time is to maximize utility.

In Fig.12, using the unity power factor, the node voltages of a IEEE 33-bus distribution network for various algorithms are shown. The 0.866 leading power factor of DGs insert into this IEEE 33-bus to obtain different curves, and the curves of node voltages are shown in Fig.13, in addition, the iteration graph of network loss about PSO-BAS and IPSO-BAS will be obtained by the optimal active power network loss of each iteration in Fig.14. The convergence speed of IPSO-BAS and PSO-BAS can be observed here. They have the fastest rate of change from the first generation to the second generation, and the value of the second generation approaches the optimal value. From the perspective of convergence speed, IPSO-BAS fully converges in the 27th generation, PSO-BAS fully converges in the 5th generation. Although IPSO-BAS gets a better value of power loss than PSO-BAS, sacrifices the speed of convergence, this trade-off is certainly worthy, because the convergence speed of IPSO-BAS is already extremely fast.

B. IEEE 69-bus radial distribution system

In order to explore the advantages of IPSO-BAS, a more complex IEEE 69-bus distribution network will be tested here, and the results of different algorithms will be studied and analyzed.

The maximum iteration of IPSO-BAS is set to 100 for case 1 and case 2. The data of line and load are given in [34]. The radial distribution system has 48 load buses, and its rated voltage is 12.66kV. The base value of power for the distribution system is 100MVA. The single-line diagram of the IEEE 69-bus distribution system is shown in Fig.26. The total load active power and reactive power of the distribution network are 3.80 MW and 2.69 MVar. The upper and lower voltage ranges of all buses are limited to 1.05 p.u. and 0.95 p.u., respectively. In order to ensure the fairness of these algorithms, there are the same conditions as on the IEEE 33-bus, three DGs with the same parameter are uniformly accessed whether the power factor is unity or 0.866 leading.

The active power loss and reactive power loss of these radial distribution system are 224.7 kW and 120.13 kVar without installation of DGs. In order to ensure the stability of the power system after inserting DGs, the ratings of DGs are limited to 0.4 p.u. to 2.0. p.u.. For each DG, their power factor will be set to unity and 0.866 leading.

Various indicators about the final result using two different cases (0.866 leading and unity) will be shown in TABLE VII and TABLE VIII, which include the location and the size of DGs, active power loss, CBN and CBV [35]. It can be known from TABLE VII, while the power factor is unity, it can be observed that there is an obvious change for the value of results on the IEEE 69-bus. The 72.06 kW is gained by IPSO-BAS, the 73.521 kW is gained by PSO-BAS, the 72.406 kW is gained by TBLO [10], the 77.100 kW is gained by LSFSA [7], the 89.000 kW is gained by GA [6], the 83.200 kW is gained by PSO [6], the 81.100 kW is gained by GA/PSO [6], the 80.91 kW is gained by GA-IWD [11]. The node voltages of IEEE 69-bus distribution system using different algorithms will be shown in Fig.27, while the power factor is unity. Here, in the condition of another power factor, about 0.866 leading power factor, the node voltages of IEEE 69-bus distribution system are shown in Fig.28.

TABLE III
THE RESULTS OF VARIOUS ALGORITHMS FOR UNITY POWER FACTOR ON THE IEEE 33-BUS DISTRIBUTION SYSTEM WITH ACTIVE POWER LOSS, PLACEMENT AND CAPACITY (MW) OF DGs, CBN, CBV.

IPSO-BAS		PSO-BAS		TBLO [10]		LSFSA [7]	
Best DG placement	Best DG capacity	Best DG placement	Best DG capacity	Best DG placement	Best DG capacity	Best DG placement	Best DG capacity
8	0.8314	8	1.0853	10	0.8246	6	1.1124
13	0.6429	13	0.5312	24	1.0311	18	0.4874
32	0.8527	32	0.5878	31	0.8862	30	0.8679

PSO [6]		GA [6]		GA/PSO [6]		GA-IWD [11]	
Best DG placement	Best DG capacity	Best DG placement	Best DG capacity	Best DG placement	Best DG capacity	Best DG placement	Best DG capacity
8	1.1768	11	1.5000	11	0.9250	11	1.2214
13	0.9816	29	0.4228	16	0.8630	16	0.6833
32	0.8297	30	1.0714	32	1.2000	32	1.2135

	IPSO-BAS	PSO-BAS	TBLO [10]	LSFSA [7]	PSO [6]	GA [6]	GA/PSO [6]	GA-IWD [11]
P_L(kW)	89.40	90.21	75.540	82.03	105.350	106.300	103.400	110.51
Reduction rate(%)	57.63	57.25	64.20	61.12	50.07	49.48	50.99	47.63
CBN	30	30	_	14	30	25	25	_
CBV(p.u.)	0.9709	0.9644	_	0.96767	0.98063	0.98094	0.98083	_

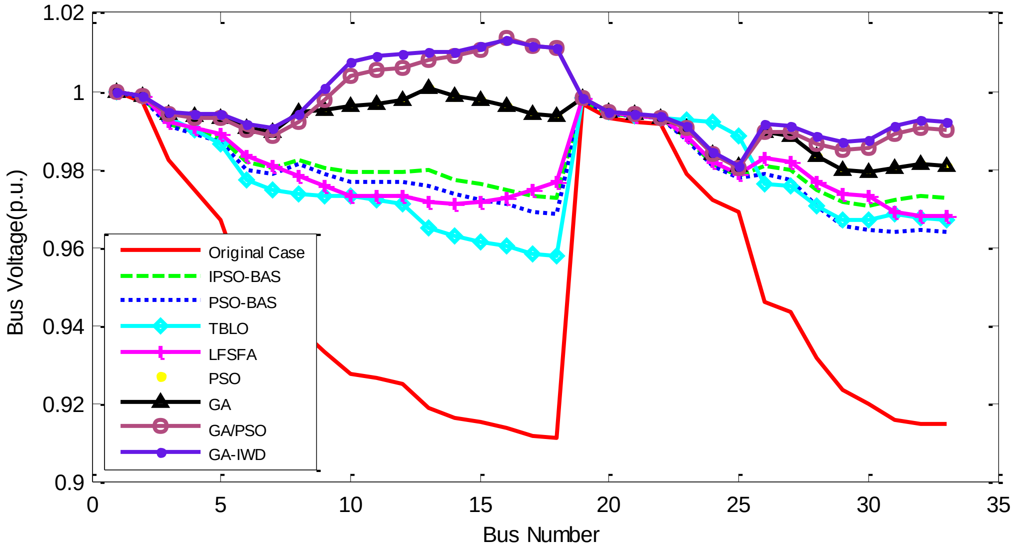

Fig.12 The node voltages for different algorithms and origin case on the IEEE 33-bus distribution network (unity power factor)

TABLE IV
THE RESULTS OF VARIOUS ALGORITHMS FOR 0.866 LEADING POWER FACTOR ON THE IEEE 33-BUS DISTRIBUTION SYSTEM WITH ACTIVE POWER LOSS, PLACEMENT AND CAPACITY OF DGs, CBN, CBV.

IPSO-BAS			PSO-BAS		
Best DG placement	Best DG capacity		Best DG placement	Best DG capacity	
	Active power (MW)	Reactive power (MVar)		Active power (MW)	Reactive power (MVar)
8	0.9087	0.5362	8	0.6192	0.5581
13	0.6192	0.5362	13	0.6192	0.5361
32	0.7563	0.5362	32	0.6192	0.5824

LSFSA [7]		
Best DG placement	Best DG capacity	
	Active power (MW)	Reactive power (MVar)
6	1.1976	0.6915
18	0.4778	0.2759
30	0.9205	0.5315

	IPSO-BAS	PSO-BAS	LSFSA
P_L(kW)	28.21	29.42	26.720
Reduction rate(%)	86.02	84.88	87.34
CBN	31	31	25
CBV(p.u.)	0.99301	0.98511	0.98266

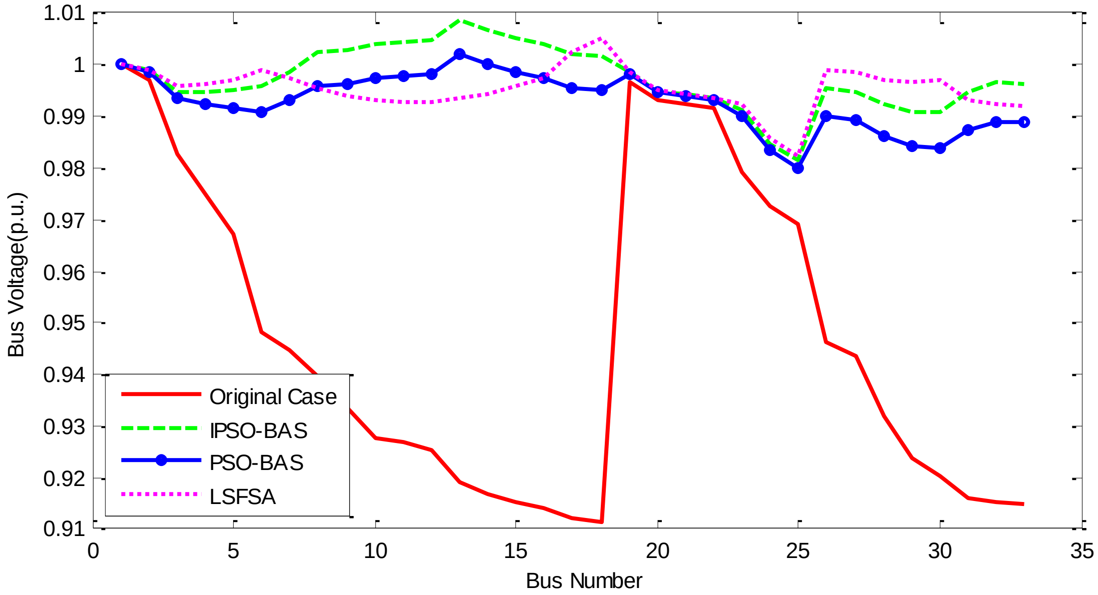

Fig.13 The node voltages for different algorithms and origin case on the IEEE 33-bus distribution network (0.866 leading power factor)

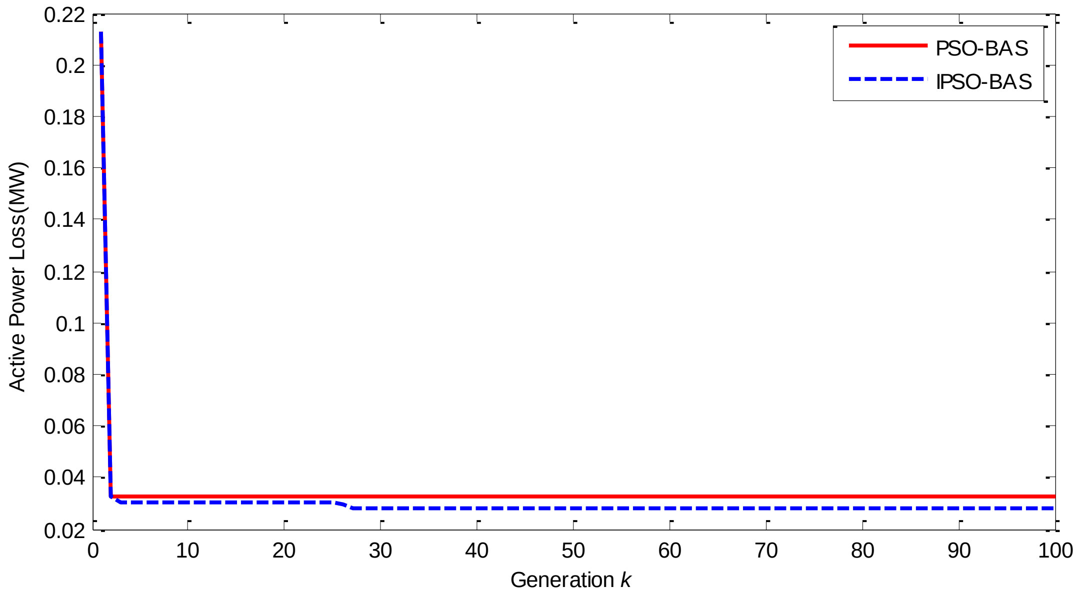

Fig.14 The active power loss convergence curves using IPSO-BAS and PSO-BAS on the IEEE 33-bus distribution network (0.866 leading power factor)

Due to the increased complexity of the node model, the value of *rate* needs to be reselected here to ensure that IPSO-BAS and PSO-BSA using 0.866 leading power factor also obtain the best results. In Fig.15 and Fig.16, it can observe that various *rate* will obtain different results for IPSO-BAS and PSO-BAS. In Fig.17, although the same result (7.602kW) is obtained by two different parameters (*rate=0.8* and *rate=0.6*) for IPSO-BAS, the convergence generation is 26th when *rate* is 0.8, then *rate* is 0.6, the convergence generation is 46th. In summary, the best result will be obtained when *rate* is 0.8.

Then, in Fig.29, the convergence speed of IPSO-BAS and PSO-BAS will be shown here, it can be known that IPSO-BAS and PSO-BAS have the fastest rate of change from the first generation to the second generation. However, the second generation value of IPSO-BAS is only half the second generation value of PSO-BAS, and the IPSO-BAS fully converges in the 26th generation, the PSO-BAS fully converges in the 52nd generation. The result of IPSO-BAS is 7.602 kW, then the result of PSO-BAS is 8.098 kW, 16.260 kW is obtained by LSFSA [7].

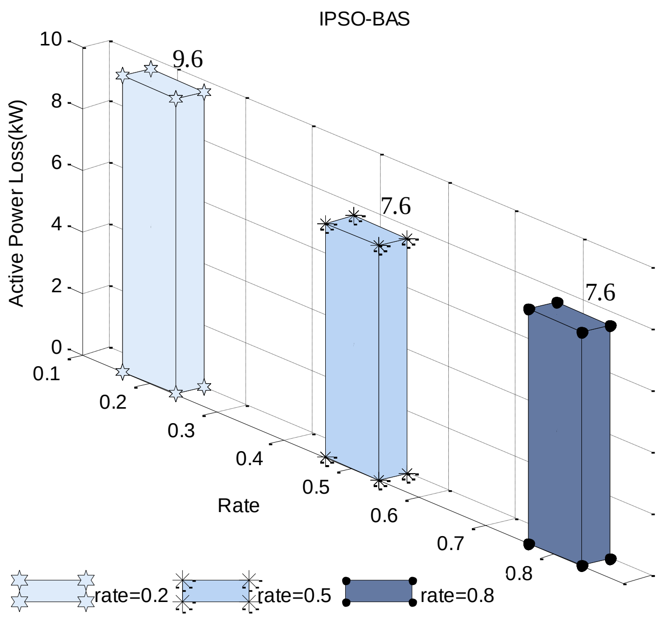

Fig.15 Active power loss using different rate for IPSO-BAS on the IEEE 69-bus system

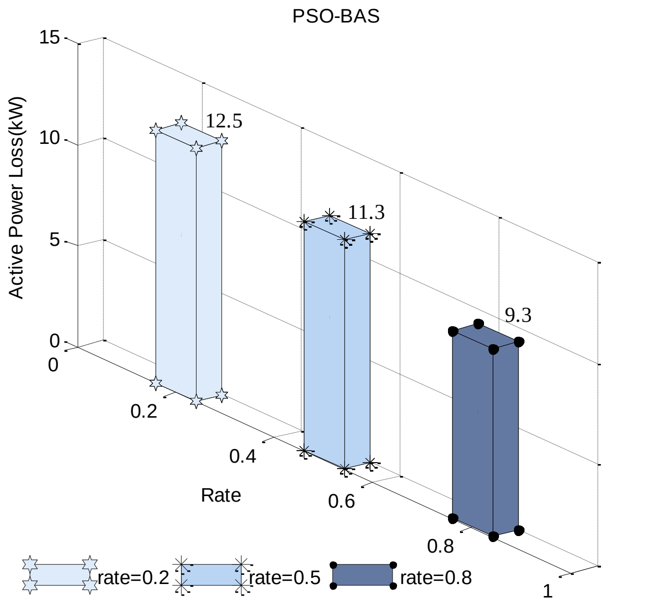

Fig.16 Active power loss using different rate for PSO-BAS on the IEEE 69-bus system

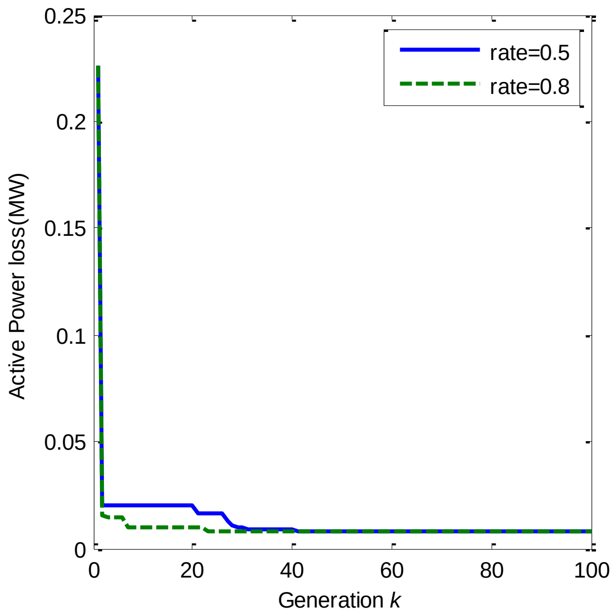

Fig.17 Convergence graph using for IPSO-BAS (0.5 and 0.8)

In addition to the above calculations on how to obtain the optimal distributed power size under the peak load, the new energy generators on the IEEE 69-bus distribution network will be introduced and a strategy for regulating the optimal network loss of the annual load is proposed.

In literature [12], there are the daily load curve of the power system load and the corresponding network power loss, and they are shown Fig.18 in and Fig.19.

In this article, three renewable energy sources are introduced as distributed power sources, namely biomass, wind energy and solar photovoltaic. Among them, the biomass power is modeled as a synchronous motor, the wind power is modeled as a double-fed induction generator (DFIG) or full-converter synchronous motors, the photovoltaic power sources are integrated using converters.

The power generation of solar photovoltaic and wind power are limited by natural factors. The power generation curve is shown in Fig.20.

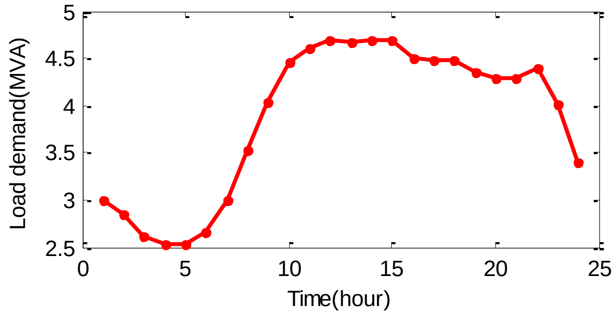

Fig.18 The daily load demand curve.

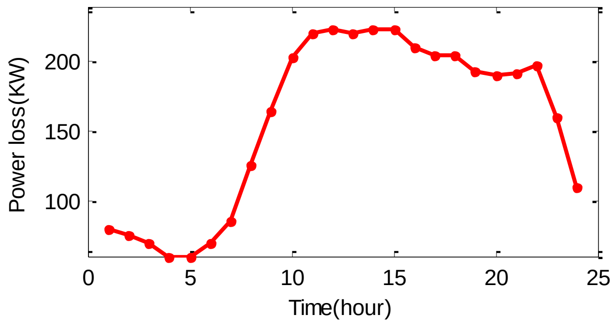

Fig.19 The daily power loss curve.

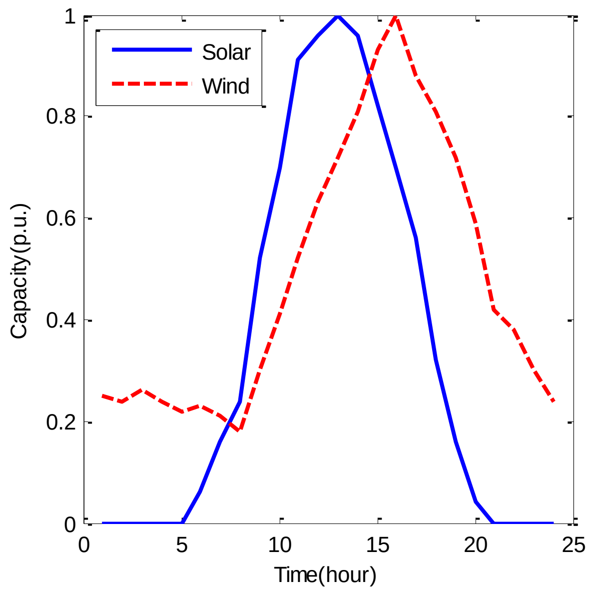

Fig.20 The daily capacity of solar and wind

On the contrary, biomass power will not be restricted by natural factors, so the size can be adjusted artificially with high flexibility.

Through the calculation and analysis of each node of the system by the IPSO-BAS algorithm, the best position of inserting node, the 61st node, is obtained. Then, for the three energy sources, they are individually inserted into the 61st node of the system, and the power generation of biomass energy is fully regulated within a controlled range. For photovoltaic and wind power sources, because they are limited by natural factors, the power generations need to be slightly adjusted according to their real-time capacity.

In the Fig.21, the adjustable size of these three renewable energy sources in 24 hours are shown here.

At the same time, in the TABLE V, it shows the annual network loss about plugging three types of renewable energy into the network and the original network. It can be observed

TABLE V
THE ANNUAL NETWORK LOSS ABOUT PLUGGING THREE TYPES OF RENEWABLE ENERGY INTO THE NETWORK AND THE ORIGINAL NETWORK

	Origin	Biomass energy		Wind energy		Solar energy	
		IPSO-BAS	Proposed method [12]	IPSO-BAS	Proposed method [12]	IPSO-BAS	Proposed method [12]
Best DG placement	–	61	61	61	61	61	61
Network loss (MWh)	1381.53	152.37	184.68	286.46	307.52	622.84	648.06

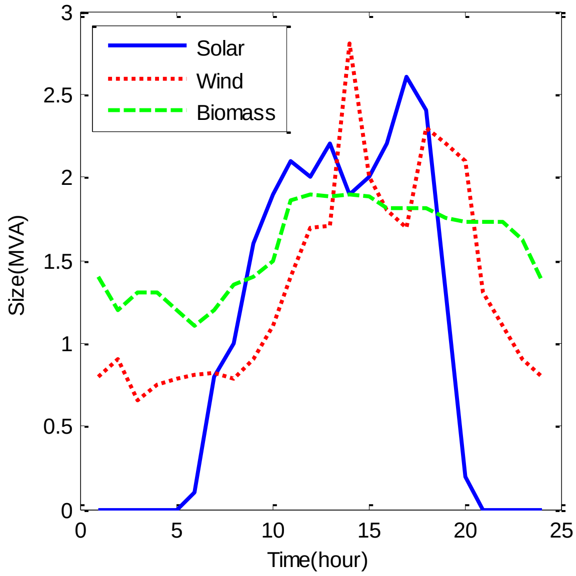

Fig.21 The size of these three renewable energy sources in one day.

here that the annual network loss value is obtained by the IPSO-BAS algorithm in this paper, which is less than the calculated annual network loss value by the method in literature [12], and it can be observed that the difference in the network loss value of biomass energy is the largest.

From the above results, it can be analyzed that adjusting the size of the generator according to the daily load curve will obtain the optimal annual network loss value. In the above case, the generator is only inserted in one node. Here, this paper will explore the position of multiple generators that can be adjusted in real time.

Because biomass energy is not restricted by natural factors and flexible regulation, this paper will study how much the annual network loss is caused by two and three biomass power sources respectively to be plugged into the IEEE 69-bus distribution network. In order to improve accuracy, here, the amount of biomass energy and network loss at each time of the day will be calculated based on the daily load curve, and the annual network loss value can be obtained through formula (2). In the TABLE VI, it will show the size of the network loss of the various cases in the year. And in the Fig.22 and Fig.23, they will show the size of the generators at each moment when two and three generators are inserted into the IEEE 69-bus system under the same total load capacity.

C. IEEE 119-bus radial distribution system

The performance of IPSO-BAS on the IEEE 69-bus has been greatly improved over the IEEE 33-bus. Here, this paper will introduce more complex model (IEEE 119-bus) to prove whether the more complex the model, the performance of IPSO-BAS will gradually improve.

About the IEEE 119-bus, this paper only explores when the power factor is 0.866 leading. The maximum iteration of IPSO-BAS is set to 100. The radial distribution network has 117 load buses, and its rated voltage is 12.66kV. The base value of power for the distribution system is 100MVA. The single-line diagram of IEEE 119-bus distribution system is shown in Fig.25. The total load active power and reactive power of the distribution network are 22.71 MW and 17.04 MVar. The upper and lower voltage ranges about all buses are limited to 1.1 p.u. and 0.9 p.u.. The node voltages for IEEE 119-bus distribution network are shown in Fig.30. The active power loss and reactive power loss of the IEEE 119-bus are 978.1 kW and 718.8 kVar without DGs. For five connected DGs, their ratings are limited to 1.0 p.u. to 5.0. p.u, and they own the same physical properties as the DGs on the IEEE 69-bus and IEEE 33-bus. 682.26 kW is obtained by PSO [6], 603.57kW is obtained by PSO-BAS, 562.86kW is obtained by IPSO-BAS. In TABLE IX, it shows the installation position and size of five DGs, active power loss, critical bus CBN and CBV. The active power loss convergence curves are shown in Fig.31.

V. STATISTICAL ANALYSIS

The comparative analysis of the data is obtained from IEEE 33-bus, IEEE 69-bus and IEEE 119-bus distribution systems to get the advantages of the IPSO-BAS algorithm. For each algorithm, node voltage can obtain stable data, here, this paper will not discuss whether IPSO-BAS and other algorithms have advantages in voltage stability, and put the main research and analysis on active power loss.

First, this paper needs to consider whether *rate* has different effects on the complexity of the data and the model.

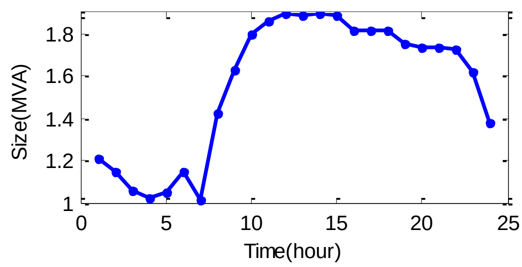

Fig.22 The total size of the two inserted biomass power sources

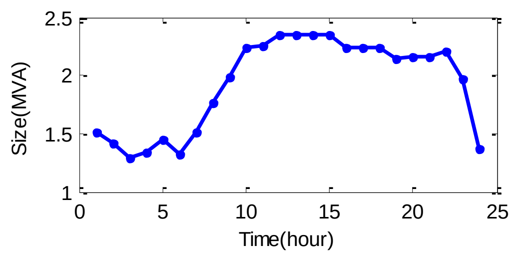

Fig.23 The total size of the three inserted biomass power sources

As can be seen from Fig.4, Fig.5, Fig.15, Fig.16 and Fig.17, the *rate* is 0.8, the optimal value or the fastest convergence speed is always obtained, so we judge that rate is equal to 0.8, and it is the optimal value of IPSO-BAS and PSO-BAS.

TABLE VI
COMPARISON OF ENERGY LOSS OF THREE SCHEMES

	One biomass	Two biomass	Three biomass
Best DG placement	61	61,63	17,61,63
Network loss (MWh)	152.37	172.12	60.55

Secondly, when the power factor is unity, the obtained result data by IPSO-BAS on the IEEE 33-bus system is obviously inferior. It can be seen that the value of IPSO-BAS is 89.40kW, although it is better than the data of PSO, GA, GA/PSO, it is obviously insufficient compared with TBLO and LSFSA, and the differences among the values are large. It can be obtained from the analysis of the result data. The gap with TBLO is 13.86kW and the gap with LSFSA is 7.37kW.

When the power factor is 0.866 leading, in other words,

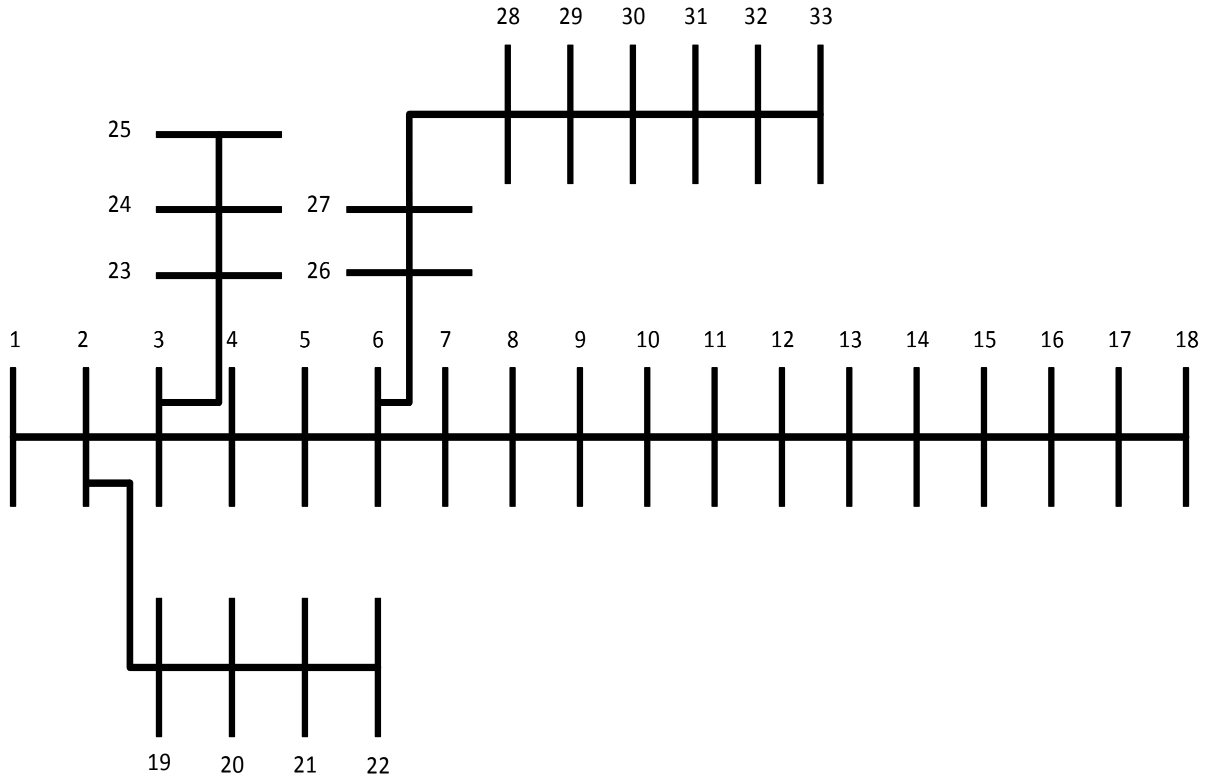

Fig.24 The schematic diagram of IEEE 33-bus radial distribution system.

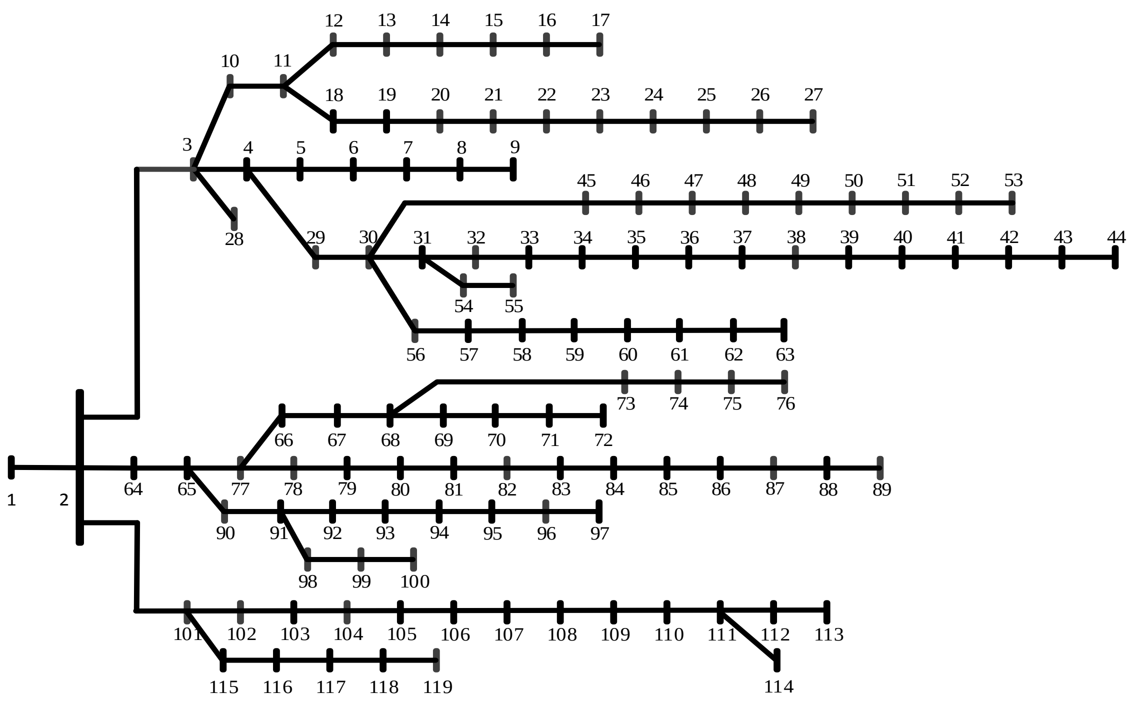

Fig.25 The schematic diagram of IEEE 119-bus radial distribution system

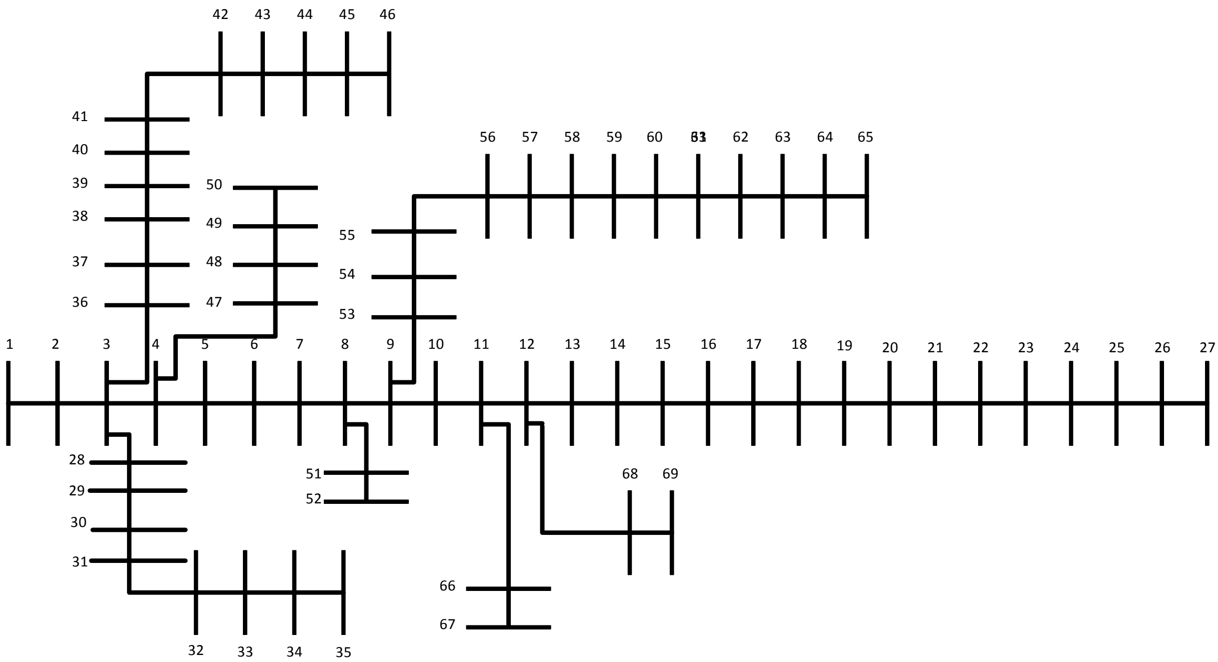

Fig.26 The schematic diagram of IEEE 69-bus radial distribution system.

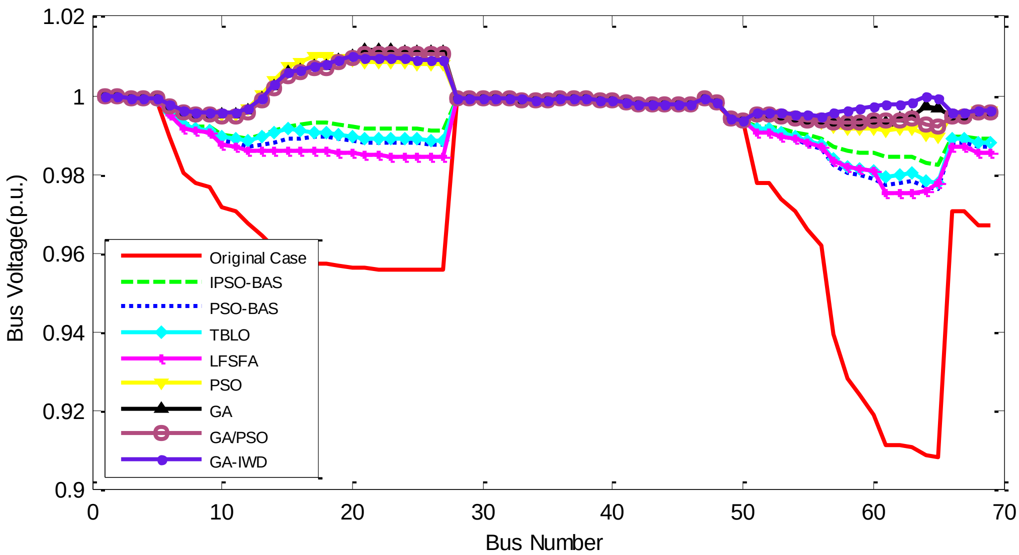

Fig.27 The node voltage for different algorithms and origin case on the IEEE 69-bus distribution network (unity power factor)

TABLE VII
THE RESULTS OF VARIOUS ALGORITHMS FOR UNITY POWER FACTOR ON THE IEEE 69-BUS DISTRIBUTION SYSTEM WITH ACTIVE POWER LOSS, PLACEMENT AND CAPACITY (MW) OF DGs, CBN, CBV.

IPSO-BAS		PSO-BAS		TBLO [10]		LFSFA [7]	
Best DG placement	Best DG capacity	Best DG placement	Best DG capacity	Best DG placement	Best DG capacity	Best DG placement	Best DG capacity
17	0.5808	17	0.5188	15	0.5919	18	0.4204
61	1.2521	61	0.6152	61	0.8188	60	1.3311
63	0.6099	63	1.0599	63	0.9003	65	0.4298

PSO [6]		GA [6]		GA/PSO [6]		GA-IWD [11]	
Best DG placement	Best DG capacity	Best DG placement	Best DG capacity	Best DG placement	Best DG capacity	Best DG placement	Best DG capacity
17	0.9925	21	0.9297	21	0.9105	64	0.8059
61	1.1998	62	1.0752	61	1.1926	61	1.3926
63	0.7956	64	0.9925	63	0.8849	20	0.9115

	IPSO-BAS	PSO-BAS	TBLO [10]	LFSFA [7]	PSO [6]	GA [6]	GA/PSO [6]	GA-IWD [11]
P_L(kW)	72.06	73.521	72.406	82.03	83.200	89.000	81.100	80.91
Reduction rate(%)	67.93	67.28	67.78	63.49	62.97	60.39	63.91	63.99
CBN	65	65	_	61	65	57	65	_
CBV(p.u.)	0.97091	0.96442	_	0.98115	0.99007	0.99360	0.99249	_

TABLE VIII
THE RESULTS OF VARIOUS ALGORITHMS FOR 0.866 LEADING POWER FACTOR ON THE IEEE 69-BUS DISTRIBUTION SYSTEM WITH ACTIVE POWER LOSS, PLACEMENT AND CAPACITY OF DGs, CBN, CBV.

IPSO-BAS			PSO-BAS		
Best DG placement	Best DG capacity		Best DG placement	Best DG capacity	
	Active power (MW)	Reactive power (MVar)		Active power (MW)	Reactive power (MVar)
17	0.5251	0.4378	17	0.5056	0.4378
61	1.2311	0.7881	61	1.1865	0.4378
63	0.5056	0.4378	63	0.5056	0.7532

LSFSA [7]		
Best DG placement	Best DG capacity	
	Active power (MW)	Reactive power (MVar)
18	0.5498	0.3175
60	1.1954	0.8635
65	0.3122	0.1803

	IPSO-BAS	PSO-BAS	LSFSA
P_L(kW)	7.602	8.098	16.260
Reduction rate(%)	96.62	96.40	92.76
CBN	60	60	61
CBV(p.u.)	0.9990	0.9971	0.9885

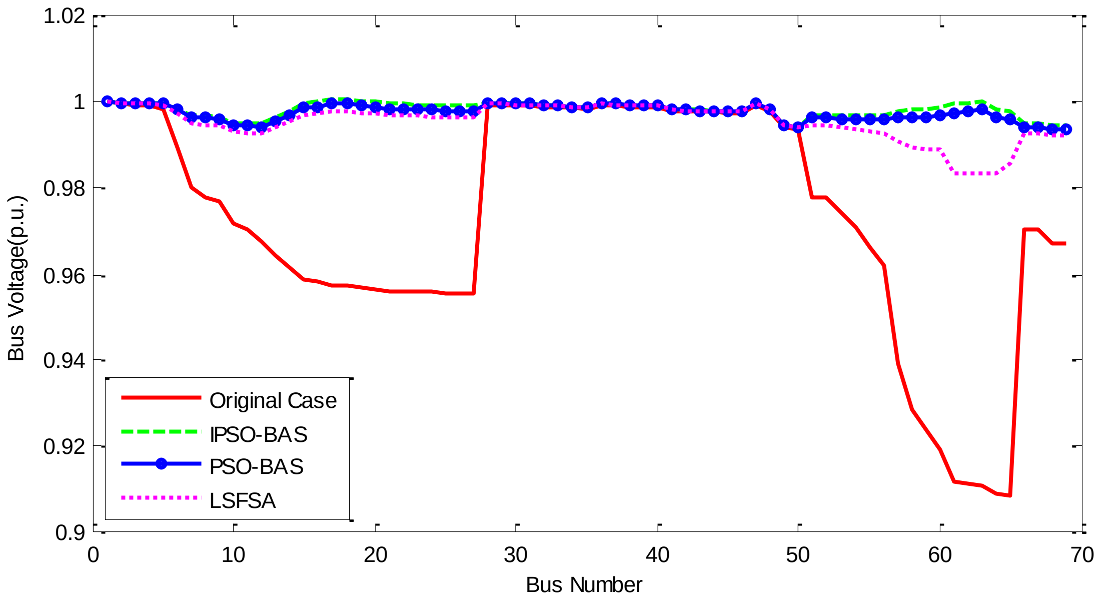

Fig.28 The node voltages for different algorithms and origin case on the IEEE 69-bus distribution network (0.866 leading power factor)

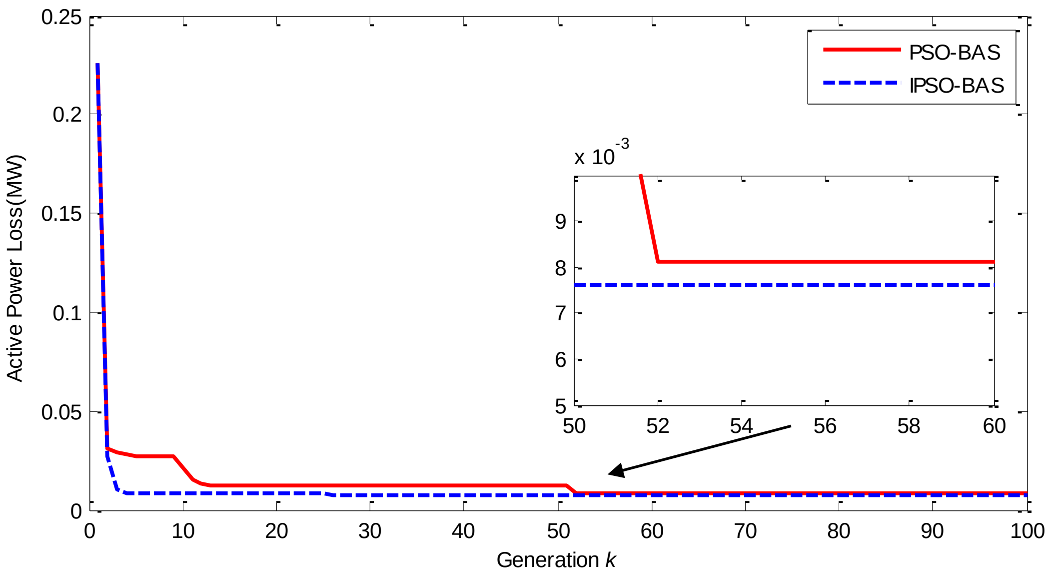

Fig.29 The active power loss convergence curves using IPSO-BAS and PSO-BAS on the IEEE 69-bus distribution network (0.866 leading power factor)

TABLE IX
THE RESULTS OF VARIOUS ALGORITHMS FOR 0.866 LEADING POWER FACTOR ON THE IEEE 119-BUS DISTRIBUTION SYSTEM WITH ACTIVE POWER LOSS, PLACEMENT AND CAPACITY OF DGs, CBN, CBV.

IPSO-BAS			PSO-BAS		
Best DG placement	Best DG capacity		Best DG placement	Best DG capacity	
	Active power (MW)	Reactive power (MVar)		Active power (MW)	Reactive power (MVar)
25	1.0010	0.6568	25	0.7690	0.6568
53	1.5778	1.5638	53	0.7584	0.6707
63	0.8577	0.6568	63	0.7599	0.6568
37	3.7919	3.0191	37	3.7893	3.2834
89	1.2397	0.6568	89	0.7592	0.6568

PSO [6]		
Best DG placement	Best DG capacity	
	Active power (MW)	Reactive power (MVar)
25	0.7959	0.6676
53	0.8203	0.6693
63	0.7709	0.7041
37	0.8057	0.6951
89	0.7967	0.6676

	IPSO-BAS	PSO-BAS	PSO
P_L(kW)	562.86	603.57	682.26
Reduction rate(%)	42.45	38.29	30.25
CBN	73	73	82
CBV(p.u.)	0.9871	0.9726	0.9833

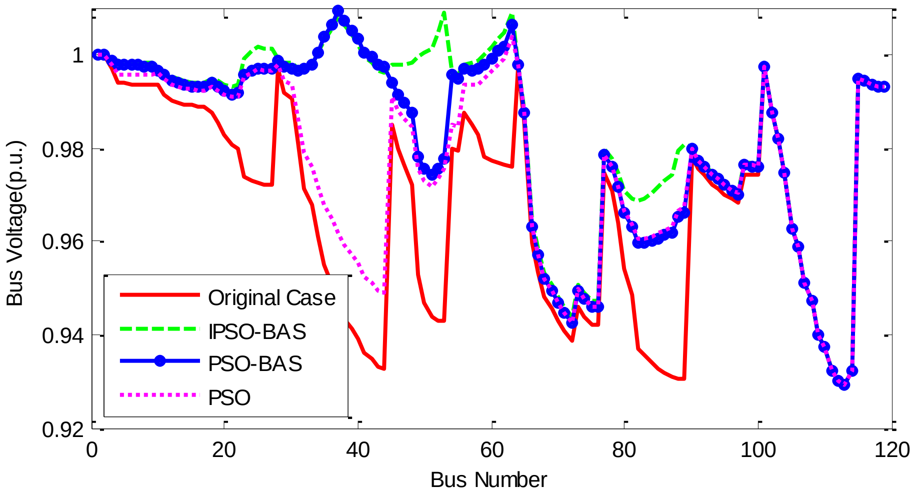

Fig.30 The node voltages for different algorithms and origin case on the IEEE 119-bus distribution network (0.866 leading power factor)

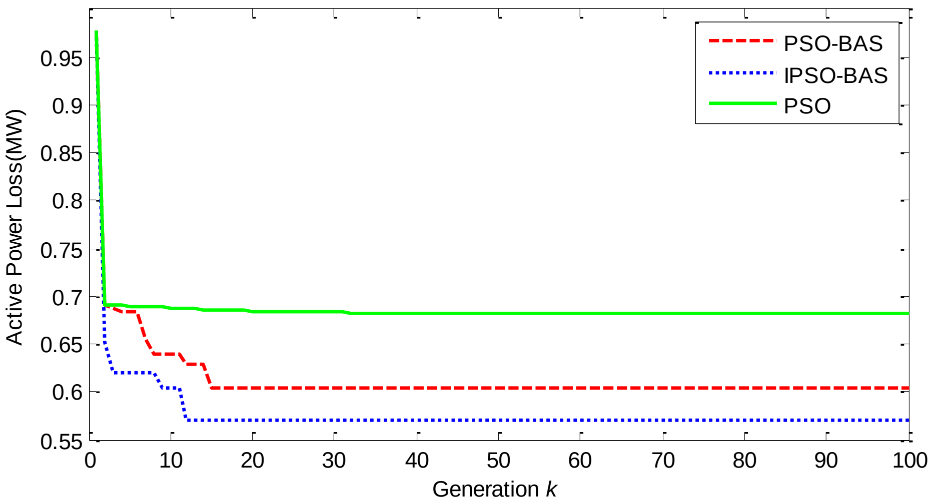

Fig.31 The active power loss convergence curves using PSO, IPSO-BAS and PSO-BAS on the IEEE 119-bus distribution network (0.866 leading power factor)

when the input variable becomes a higher dimension (both active and reactive power), the performance of IPSO-BAS is significantly improved. Although the result value is still not better than LSFSA, it can be seen that the gap between the two algorithms is reduced, and the gap is 2.781kW.

Next, when the power system model is changed from IEEE 33-bus to IEEE 69-bus, the complexity of the model increases. At the same time, it can also be observed that the performance of IPSO-BAS has also been significantly improved. When the power factor is unity, IPSO-BAS obtains the smallest active power loss, the value is 72.06kW.

When the complexity of input variable increases again, the power factor is 0.866 leading, IPSO-BAS shows more performance advantages, its power loss is 7.6kW, and the power loss of LSFSA is 16.260kW, the best result is obtained by IPSO-BAS, and it is only half the size of LSFSA.

When the network model transitioned from IEEE 69-bus to IEEE 119-bus, active power loss of the entire system has also increased from 224.7 to 978.1, nearly 4 times. In such a high power loss system, IPSO-BAS still maintains the best performance, and it is far superior to PSO using 0.866 leading power factor. The difference between their results exceeds 100kW.

Finally, the results of IPSO-BAS and PSO-BAS will be compared to analyze the performance of the improvement measures. From TABLE III, TABLE IV, TABLE VII, TABLE VIII and TABLE IX, it can be analyzed that the value of PSO-BAS has always been inferior to IPSO-BAS.

When the power factor is 0.866 leading, the convergence speed of PSO-BAS is faster than IPSO-BAS on the IEEE 33-bus, but when the complexity of the model increases, the convergence speed of IPSO-BAS is significantly faster than PSO-BAS on the IEEE 69-bus distribution network. Especially on the IEEE 119-bus, IPSO-BAS not only has a faster convergence speed than PSO-BAS, but its active power loss is also 40.71kW smaller than PSO-BAS.

In addition, this article also deeply explores the use of new energy power supplies on the IEEE 69-bus network and proposes a plan to obtain the optimal annual network loss. Under the same total capacity, this article inserts 1, 2, and 3 biomass energies into the IEEE 69-bus distribution network to verify the superiority of the proposed method. According to Fig.21, Fig.22 and Fig.23, it can be seen that the trend of the total capacity curve of the three schemes is roughly similar, but a closer look can reveal that the three energy schemes are inserted at each moment, the total energy capacity is significantly larger than the other two schemes, ranging from 1.2 to 2.4, but the annual energy loss of inserting three energy sources is the smallest, and the value is 60.55MWh, which is about 100MWh less than the other two schemes.

VI. Conclusion

It can be obtained from the above data analysis that IPSO-BAS has poor performance on simple models with low dimensions, but the dimensions and model complexity increase, the performance of the IPSO-BAS algorithm has been significantly improved. From TABLE III and TABLE IV, they show that when the power factor is unity, the result value of IPSO-BAS is not ideal, and it differs greatly from the optimal value. When the power factor is 0.866 leading (both reactive power and active power), the result value of IPSO-BAS is still not the optimal value, but the gap with the optimal value has been significantly reduced. It can be observed from TABLE VII and TABLE VIII that regardless of the power factor is unity or 0.866 leading, the value of IPSO-BAS has achieved the optimal value. In TABLE IX, IPSO-BAS still maintain the best result value, and there is a further improvement in the numerical gap

As can be seen from Fig.14, although the improvement measures achieved better results on the IEEE 33-bus distribution network, IPSO-BAS sacrificed the convergence speed. In Fig.29, on the IEEE 69-bus distribution network, it can be seen that the convergence speed has been significantly improved than before, and the numerical value does also not effect, the size is still the optimal value. In Fig.31, the performance of IPSO-BAS is significantly better than PSO-BAS on the IEEE 119-bus, and the difference in their reduction rate of active power loss increases from 0.22% to 4.16%.

As can be seen from the above summary, the IPSO-BAS algorithm has extremely fast convergence speed, strong search range capabilities, and the extremely obvious advantages in high-dimensional complex problems. Hence, the algorithm can be generalized to higher-dimensional or more complex problems.

In addition to explore the performance of IPSO-BAS, this article also proposes a scheme to optimize the annual energy loss value. The optimal installation position and size by the IPSO-BAS algorithm is used to insert 1, 2, and 3 biomass energy sources respectively.

According to the above data analysis, it can be known that inserting three biomass energy sources will obtain the best annual energy loss value, but it also requires the largest total energy capacity. If biomass energy can be changed in real time, then the real-time optimal total energy loss value will be obtained. The size of biomass energy only changes in every hour of 24 hours, and the obtained optimal network loss value is also based on this situation to estimate the annual energy loss value, but through comparative analysis, it is determined that the optimal result will be obtained by inserting three biomass energy sources at the same time, which provides the basis for the subsequent real-time regulation.

References

[1]. M.M. Othman, W. El-Khattam, Y.G. Hegazy, and A.Y. Abdelaziz, "Optimal placement and sizing of voltage controlled distributed generators in unbalanced distribution networks using supervised firefly algorithm," *International Journal of Electrical Power & Energy Systems*, vol. 82, pp. 105-113, 2016.

[2]. P.A. Gkaidatzis, A.S. Bouhouras, D.I. Doukas, K.I. Sgouras, and D.P. Labridis, "Load variations impact on optimal DG placement problem concerning energy loss reduction," *Electric Power Systems Research*, vol. 152, pp. 36-47, 2017.

[3]. G. Guo, J. Qian and S. Li, "Optimal power flow based on novel multi-objective artificial fish swarm algorithm," *Engineering Letters*, vol. 28, no. 2, pp. 542-550, 2020.

[4]. A. Ahmed, M.F. Nadeem, I.A. Sajjad, R. Bo, I.A. Khan, and A. Raza, "Probabilistic generation model for optimal allocation of wind DG in distribution systems with time varying load models," *Sustainable Energy, Grids and Networks*, vol. 22, article. 100358 (1-12), 2020.

[5]. R. Rajaram, K.S. Kumar and N. Rajasekar, "Power system reconfiguration in a radial distribution network for reducing losses and to improve voltage profile using modified plant growth simulation algorithm with Distributed Generation (DG)," *Energy Reports*, vol. 1, pp. 116-122, 2015.

[6]. M.H. Moradi and M. Abedini, "A combination of genetic algorithm and particle swarm optimization for optimal DG location and sizing in distribution systems," *International Journal of Electrical Power & Energy Systems*, vol. 34, no. 1, pp. 66-74, 2012.

[7]. S.K. Injeti and N.P. Kumar, "A novel approach to identify optimal access point and capacity of multiple DGs in a small, medium and large scale radial distribution systems," *International Journal of Electrical Power & Energy Systems*, vol. 45, no. 1, pp. 142-151, 2013.
[8]. M.C.V. Suresh and J.B. Edward, "A hybrid algorithm based optimal placement of DG units for loss reduction in the distribution system," *Applied Soft Computing*, vol. 91, article. 106191 (1-15), 2020.
[9]. A.A. El-Fergany, "Optimal capacitor allocations using evolutionary algorithms," *IET Generation, Transmission & Distribution*, vol. 7, no. 6, pp. 593-601, 2013.
[10]. S. Sultana and P.K. Roy, "Multi-objective quasi-oppositional teaching learning based optimization for optimal location of distributed generator in radial distribution systems," *International Journal of Electrical Power & Energy Systems*, vol. 63, pp. 534-545, 2014.
[11]. M.H. Moradi and M. Abedini, "A novel method for optimal DG units capacity and location in Microgrids," *International Journal of Electrical Power & Energy Systems*, vol. 75, pp. 236-244, 2016.
[12]. D.Q. Hung, N. Mithulananthan and R.C. Bansal, "Analytical strategies for renewable distributed generation integration considering energy loss minimization," *Applied Energy*, vol. 105, pp. 75-85, 2013.
[13]. T. Yuvaraj and K. Ravi, "Multi-objective simultaneous DG and DSTATCOM allocation in radial distribution networks using cuckoo searching algorithm," *Alexandria Engineering Journal*, vol. 57, no. 4, pp. 2729-2742, 2018.
[14]. D.B. Prakash and C. Lakshminarayana, "Multiple DG placements in distribution system for power loss reduction using PSO algorithm," *Procedia Technology*, vol. 25, pp. 785-792, 2016.
[15]. G. Chen, Z. Lu, Z. Zhang, and Z. Sun, "Research on hybrid modified cuckoo search algorithm for optimal reactive power dispatch problem," *IAENG International Journal of Computer Science*, vol. 45, no. 2, pp. 328-339, 2018.
[16]. G. Chen, J. Qian, Z. Zhang, and Z. Sun, "Multi-objective Improved Bat Algorithm for optimizing fuel cost, emission and active power loss in power system," *IAENG International Journal of Computer Science*, vol. 46, no. 1, pp. 118-133, 2019.
[17]. K.H. Truong, P. Nallagownden, I. Elamvazuthi, and D.N. Vo, "A Quasi-Oppositional-Chaotic Symbiotic Organisms Search algorithm for optimal allocation of DG in radial distribution networks," *Applied Soft Computing*, vol. 88, article. 106067 (1-25), 2020.
[18]. O.A. Zongo and A. Oonsivilai, "Optimal placement of distributed generator for power loss minimization and voltage stability improvement," *Energy Procedia*, vol. 138, pp. 134-139, 2017.
[19]. A.M. Imran, M. Kowsalya and D.P. Kothari, "A novel integration technique for optimal network reconfiguration and distributed generation placement in power distribution networks," *International Journal of Electrical Power & Energy Systems*, vol. 63, pp. 461-472, 2014.
[20]. X. Yuan, B. Zhang, P. Wang, J. Liang, Y. Yuan, Y. Huang, and X. Lei, "Multi-objective optimal power flow based on improved strength Pareto evolutionary algorithm," *Energy*, vol. 122, pp. 70-82, 2017.
[21]. P.D. Huy, V.K. Ramachandaramurthy, J.Y. Yong, K.M. Tan, and J.B. Ekanayake, "Optimal placement, sizing and power factor of distributed generation: A comprehensive study spanning from the planning stage to the operation stage," *Energy*, vol. 195, article. 117011 (1-23), 2020.
[22]. R. Barbieri, N. Barbieri and K.F. de Lima, "Some applications of the PSO for optimization of acoustic filters," *Applied Acoustics*, vol. 89, pp. 62-70, 2015.
[23]. D.B. Prakash and C. Lakshminarayana, "Multiple DG placements in distribution system for power loss reduction using PSO algorithm," *Procedia Technology*, vol. 25, pp. 785-792, 2016.
[24]. Y. Li and F. Li, "PSO-based growing echo state network," *Applied Soft Computing*, vol. 85, article. 105774 (1-10), 2019.
[25]. B. Bhattacharyya and S. Raj, "PSO based bio inspired algorithms for reactive power planning," *International Journal of Electrical Power & Energy Systems*, vol. 74, pp. 396-402, 2016.
[26]. M.A.H. Akhand, S. Akter, M.A. Rashid, and S.B. Yaakob, "Velocity tentative PSO: An optimal velocity implementation based particle swarm optimization to solve traveling salesman problem," *IAENG International Journal of Computer Science*, vol. 42, no. 3, pp. 221-232, 2015.
[27]. J. Niu, Y. Zhang and Z. Li, "Quantum-behaved particle swarm optimization algorithm based on dynamic dual-population joint-search mechanism," *IAENG International Journal of Computer Science*, vol. 46, no. 4, pp. 734-749, 2019.
[28]. J. Wang, W. Wang, Z. Yuan, H. Wang, and J. Wu, "A chaos disturbed beetle antennae search algorithm for a multiobjective distribution network reconfiguration considering the variation of load and DG," *IEEE Access*, vol. 8, pp. 97392-97407, 2020.
[29]. M. Lin, Q. Li, F. Wang, and D. Chen, "An improved beetle antennae search algorithm and its application on economic load distribution of power system," *IEEE Access*, vol. 8, pp. 99624-99632, 2020.
[30]. M.A. Kashem, V. Ganapathy, G.B. Jasmon, and M.I. Buhari, "A novel method for loss minimization in distribution networks," in *International Conference on Electric Utility Deregulation and Restructuring and Power Technologies*, London, 2000, pp. 251-256.
[31]. T.P. Nguyen and D.N. Vo, "A novel stochastic fractal search algorithm for optimal allocation of distributed generators in radial distribution systems," *Applied Soft Computing*, vol. 70, pp. 773-796, 2018.
[32]. S. Sharma, S. Bhattacharjee and A. Bhattacharya, "Quasi-Oppositional Swine Influenza Model Based Optimization with Quarantine for optimal allocation of DG in radial distribution network," *International Journal of Electrical Power & Energy Systems*, vol. 74, pp. 348-373, 2016.
[33]. U. Raut and S. Mishra, "An improved sine–cosine algorithm for simultaneous network reconfiguration and DG allocation in power distribution systems," *Applied Soft Computing*, vol. 92, article. 106293 (1-55), 2020.
[34]. M. Chakravorty and D. Das, "Voltage stability analysis of radial distribution networks," *Int. J. Electr. Power Energy Syst*, vol. 23, no. 2, pp. 129-135, 2001.
[35]. S. Sultana and P.K. Roy, "Krill herd algorithm for optimal location of distributed generator in radial distribution system," *Applied Soft Computing*, vol. 40, pp. 391-404, 2016.